

Corrosion behaviors of $\text{Fe}_{45-x}\text{Cr}_{18}\text{Mo}_{14}\text{C}_{15}\text{B}_6\text{Y}_2\text{M}_x$ ($\text{M} = \text{Al}, \text{Co}, \text{Ni}, \text{N}$ and $x = 0, 2$) bulk metallic glasses under conditions simulating fuel cell environment

J. Jayaraj^b, Y.C. Kim^a, K.B. Kim^a, H.K. Seok^a, E. Fleury^{a,*}

^a Advanced Metals Research Center, Korea Institute of Science and Technology (KIST), P.O. Box 131, Cheongryang, Seoul 130-650, Republic of Korea

^b International R&D Academy, KIST-University of Science and Technology, P.O. Box 131, Cheongryang, Seoul 130-650, Republic of Korea

Available online 29 September 2006

Abstract

The corrosion properties of the $\text{Fe}_{45-x}\text{Cr}_{18}\text{Mo}_{14}\text{C}_{15}\text{B}_6\text{Y}_2\text{M}_x$ (with $\text{M} = \text{Al}, \text{Co}, \text{Ni}, \text{N}$ and $x = 0, 2$) bulk metallic glasses have been investigated in a 1 M $\text{H}_2\text{SO}_4 + 2$ ppm F^- solution at 80 °C with H_2 and air bubbling, which simulate environments of the polymer electrolyte membrane fuel cell. The partial replacement of 2 at.% Fe led to significant modification of the corrosion behavior and resulted in corrosion resistances superior to that of stainless steel.

© 2006 Elsevier B.V. All rights reserved.

Keywords: Amorphous materials; Corrosion; Electrochemical reactions

1. Introduction

Among the existing metallic amorphous alloys, the Fe-based bulk metallic glasses (BMGs) emerged as the most attractive systems owing to their combination of remarkable properties particularly the elevated glass transition temperature, high hardness, high strength and high corrosion resistance in HCl environments [1–4]. Recently, we introduced a novel idea of using Fe-BMGs as bipolar plates in polymer electrolyte membrane fuel cell (PEMFC) [5]. In addition to properties such as electrical conductivity, strength and non-permeability to gases, materials for bipolar plates should be highly corrosion resistant. The preliminary study demonstrated the effect of major elements such as Cr and Mo on the corrosion properties. The aim of this paper is to report the effect of minor alloying elements on the corrosion behavior. The dependence of the corrosion properties of the $\text{Fe}_{45-x}\text{Cr}_{18}\text{Mo}_{14}\text{C}_{15}\text{B}_6\text{Y}_2\text{M}_x$ BMGs for $\text{M} = \text{Al}, \text{Co}, \text{Ni}, \text{N}$ and $x = 0, 2$ under conditions that simulate bipolar plate PEMFC environments will be demonstrated by means of potentiodynamic and potentiostatic polarization tests.

2. Experimental procedure

Starting with a composition developed by Ponnambalam et al. [6], $\text{Fe}_{45-x}\text{Cr}_{18}\text{Mo}_{14}\text{C}_{15}\text{B}_6\text{Y}_2\text{M}_x$ (with $\text{M} = \text{Al}, \text{Co}, \text{Ni}, \text{N}$ and $x = 0, 2$) alloys were prepared by arc melting of high purity metals and Fe–Cr–N master alloy under an argon atmosphere. Plates of dimension 1.2 mm × 5 mm × 50 mm were prepared by copper mold casting. The amorphous nature of the alloys was checked by X-ray diffraction. As shown in Fig. 1, the XRD traces display broad peaks around 45° characteristics of the amorphous structure. Potentiodynamic and potentiostatic tests were performed on carefully polished with 1200 grit SiC paper and ultrasonically cleaned BMG and stainless steel SUS316L plates under conditions that simulate PEMFC anodic and cathodic environments [7]. Further details on the corrosion tests can be found in ref. [5].

3. Results

3.1. Potentiodynamic behavior of Fe-based BMGs and stainless steel

Fig. 2(a) shows the polarization curves obtained for the BMGs and SUS316L in solution with H_2 bubbling, simulating the PEMFC anodic environment. The main difference in the corrosion behavior consists in the position of the corrosion potential, E_{corr} . $\text{Fe}_{43}\text{Cr}_{18}\text{Mo}_{14}\text{C}_{15}\text{B}_6\text{Y}_2\text{Al}_2$ and SUS316L have negative values while other BMGs have positive E_{corr} values. Considering the potential of -0.1 V corresponding to the operating potential at the PEMFC anode, the passivation current densities

* Corresponding author. Tel.: +82 2 958 5456; fax: +82 2 958 5449.
E-mail address: efleury@kist.re.kr (E. Fleury).

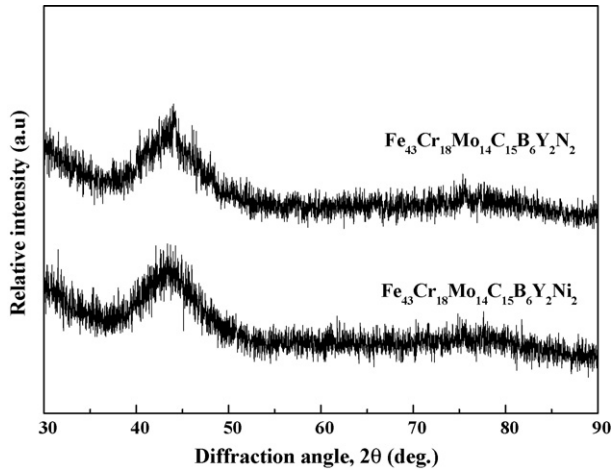
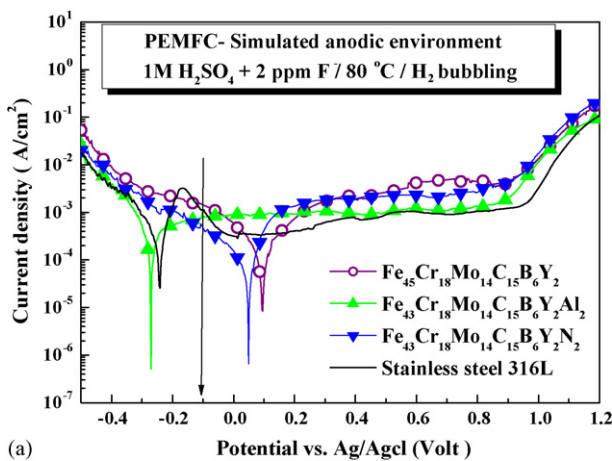
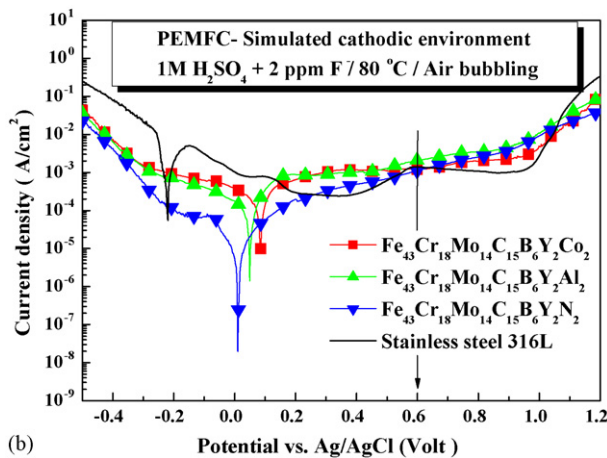


Fig. 1. XRD traces of $\text{Fe}_{43}\text{Cr}_{18}\text{Mo}_{14}\text{C}_{15}\text{B}_6\text{Y}_2\text{Al}_2$ and $\text{Fe}_{43}\text{Cr}_{18}\text{Mo}_{14}\text{C}_{15}\text{B}_6\text{Y}_2\text{Ni}_2$ metallic glasses.

for all alloys are almost similar but $\text{Fe}_{43}\text{Cr}_{18}\text{Mo}_{14}\text{C}_{15}\text{B}_6\text{Y}_2\text{Ni}_2$ had the lowest value of about 0.42 mA cm^{-2} . The BMGs passivated spontaneously whereas the stainless steel exhibited an active-passive transition behavior, which means that the



(a)



(b)

Fig. 2. Potentiodynamic polarization in $1 \text{ M H}_2\text{SO}_4 + 2 \text{ ppm F}^-$ at 80°C : (a) with H_2 bubbling simulating the anodic environment and (b) with air bubbling simulating the cathodic environment of PEMFC.

passive layers of the BMGs are more stable than that of SUS316L. In view of the corrosion current density (I_{corr}) estimated from the polarization curves by the Tafel slope method [8], the corrosion resistance of the alloys follows the order: SUS316L ($I_{\text{corr}} = 1.51 \text{ mA cm}^{-2}$) < $\text{Fe}_{43}\text{Cr}_{18}\text{Mo}_{14}\text{C}_{15}\text{B}_6\text{Y}_2\text{Co}_2$ (1.34) < $\text{Fe}_{45}\text{Cr}_{18}\text{Mo}_{14}\text{C}_{15}\text{B}_6\text{Y}_2$ (0.68) < $\text{Fe}_{43}\text{Cr}_{18}\text{Mo}_{14}\text{C}_{15}\text{B}_6\text{Y}_2\text{Ni}_2$ (0.57) < $\text{Fe}_{43}\text{Cr}_{18}\text{Mo}_{14}\text{C}_{15}\text{B}_6\text{Y}_2\text{Al}_2$ (0.43) < $\text{Fe}_{43}\text{Cr}_{18}\text{Mo}_{14}\text{C}_{15}\text{B}_6\text{Y}_2\text{Al}_2$ (0.11).

Fig. 2(b) shows the polarization curves obtained in solution with air bubbling, which simulate the PEMFC cathodic condition. For the $\text{Fe}_{43}\text{Cr}_{18}\text{Mo}_{14}\text{C}_{15}\text{B}_6\text{Y}_2\text{Al}_2$ BMG, the E_{corr} increased meaning that the alloy is nobler under air bubbling in comparison to H_2 bubbling. At the potential of 0.6 V, corresponding to the operating potential of the PEMFC cathode, the passivation current density is the lowest for the $\text{Fe}_{43}\text{Cr}_{18}\text{Mo}_{14}\text{C}_{15}\text{B}_6\text{Y}_2\text{Ni}_2$ BMG with value of about 1.5 mA cm^{-2} . Considering the I_{corr} in the cathodic environment, the corrosion resistance of the alloy follows the order: SUS316L (3.26) < $\text{Fe}_{43}\text{Cr}_{18}\text{Mo}_{14}\text{C}_{15}\text{B}_6\text{Y}_2\text{Co}_2$ (0.53) < $\text{Fe}_{45}\text{Cr}_{18}\text{Mo}_{14}\text{C}_{15}\text{B}_6\text{Y}_2$ (0.38) < $\text{Fe}_{43}\text{Cr}_{18}\text{Mo}_{14}\text{C}_{15}\text{B}_6\text{Y}_2\text{Al}_2$ (0.09) < $\text{Fe}_{43}\text{Cr}_{18}\text{Mo}_{14}\text{C}_{15}\text{B}_6\text{Y}_2\text{Ni}_2$ (0.024) < $\text{Fe}_{43}\text{Cr}_{18}\text{Mo}_{14}\text{C}_{15}\text{B}_6\text{Y}_2\text{Ni}_2$ (0.016). For BMGs, these values were lower than those recorded under H_2 bubbling. The higher corrosion resistance of Fe-BMGs under air bubbling reflects the positive effect of the air (i.e., oxygen) on the formation of the passive layers. These results indicated that Fe-BMGs have higher corrosion resistance than SUS316L in PEMFC environment and that the corrosion properties are sensitive to minor modification of the alloy compositions.

3.2. Potentiostatic behavior of Fe-based amorphous alloy

The stability of the passive layers was studied by potentiostatic polarization tests in simulated PEMFC environment for 2 h. Fig. 3(a) shows that, under a constant applied potential of 0.6 V in solution with air bubbling, the current density decreased rapidly to reach low values. This reduction of the current den-

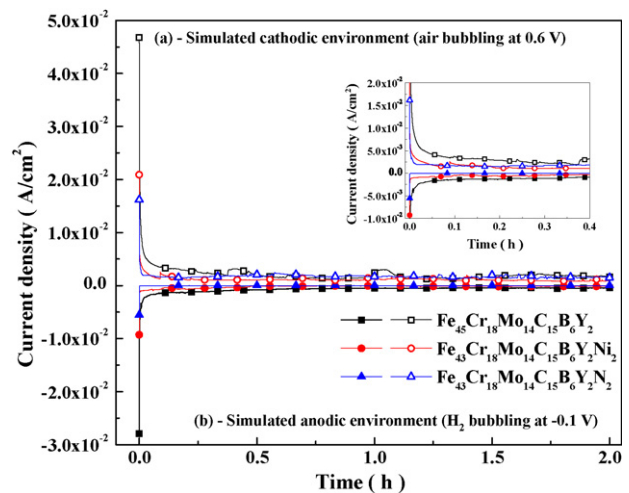


Fig. 3. Potentiostatic polarization in $1 \text{ M H}_2\text{SO}_4 + 2 \text{ ppm F}^-$ at 80°C : (a) H_2 bubbling simulating the cathodic environment and (b) air bubbling simulating the anodic environment of PEMFC.

sity reflects the passivation behavior of the films formed on the surfaces of the Fe-BMGs under such environment.

With the exception of $\text{Fe}_{43}\text{Cr}_{18}\text{Mo}_{14}\text{C}_{15}\text{B}_6\text{Y}_2\text{Al}_2$ BMG [5], in solution with H_2 bubbling and a constant applied voltage of -0.1 V (Fig. 3(b)), the initial current was negative because the corrosion potentials were larger than the applied -0.1 V potential. The negative current densities increased rapidly at the very first stage of polarization and after a short time tended to reach low values. The negative current indicated that the passive layers were cathodically protected, which means there was no active dissolution of the BMGs. The time required to reach stabilization as well as the final values of the current density are dependent on the alloy composition, which suggests a strong influence of the minor elements on the thickness and composition of the passive layers.

4. Discussion

In the late 1970s, and early 1980s, Hashimoto [3] demonstrated the high corrosion properties of Fe-based amorphous alloys in HCl environments. Similar to the effect observed for stainless steel, Cr is one of the key passivating elements responsible for the high corrosion resistance of Fe-based metallic glasses [4]. Jayaraj et al. [5] have shown that, for identical Cr content, Fe-BMGs have superior corrosion properties than SUS316L in conditions simulating cathodic and anodic PEMFC environments. In Fe-BMGs, Mo is necessary for the formation of the amorphous phase. However, as demonstrated by Pang et al. [4], the excess of Mo degraded the corrosion properties in HCl solution. This dependence was confirmed under simulated PEMFC environments and the best corrosion properties were obtained for an alloy with 8 at.% Mo [5]. Also XPS analyses indicated that the passive films were essentially composed by Cr_2O_3 covering Fe_2O_3 and MoO oxides [5].

In the present work, the potentiodynamic studies under simulated PEMFC environment indicated that the replacement of 2 at.% of Fe by elements such as Al, Ni and N provided significant enhancement of the corrosion resistance. The $\text{Fe}_{43}\text{Cr}_{18}\text{Mo}_{14}\text{C}_{15}\text{B}_6\text{Y}_2\text{Al}_2$ show higher corrosion resistance in anodic environment while $\text{Fe}_{43}\text{Cr}_{18}\text{Mo}_{14}\text{C}_{15}\text{B}_6\text{Y}_2\text{N}_2$ exhibited a significantly higher corrosion resistance in cathodic environment. The reason why the elements resulted in better corrosion resistance in these particular environments is not clear yet. However, it is well known that, Al and Ni tend to form highly protective Al_2O_3 and NiO oxides. By replacing Fe, which forms

a porous oxide layer, it is believed that they tend to reduce the corrosion reaction by forming impervious oxide layers protecting more efficiently the underlying amorphous matrix.

The effect of N on the corrosion resistance follows a different mechanism. In contrast to Al, Ni and Co elements, N in the alloy is negatively charged like N^- . So if negatively charged N^- ions are present in the passive film, they will repel the SO_4^- and F^- ions, which would result in a decrease of the corrosion reaction and corrosion current [9]. Moreover, owing to the presence of Mo, a synergetic effect between Mo and N elements on the corrosion properties is believed to have an active role, as demonstrated on conventional Fe-based alloys [9]. Further analyses are currently in progress to determine the exact role of Al, Ni and N on the formation of the passive layers.

5. Conclusion

This work emphasizes the effect of minor alloying elements on the corrosion properties of Fe-based BMGs in conditions simulating the PEMFC environments. The partial replacement of Fe by Al resulted in high corrosion resistance in solution with H_2 bubbling, while N provided significantly higher corrosion properties under air bubbling. Furthermore, the potentiodynamic studies under PEMFC environments demonstrated the superior corrosion properties of the Fe-based BMGs in comparison to that of the SUS316L.

Acknowledgement

This work was financially supported by KIST research program #2E18470.

References

- [1] A. Inoue, Bulk Amorphous Alloys—Practical Characteristics and Applications, Trans Tech Publications Inc., Enfield, USA, 1999, p. 83.
- [2] T.D. Shen, R.B. Schwarz, Appl. Phys. Lett. 75 (1) (1999) 49–51.
- [3] K. Hashimoto, in: F.E. Luborsky (Ed.), Amorphous Metallic Alloys, Butterworths Monographs in Materials, 1983, pp. 471–486.
- [4] S. Pang, T. Zhang, K. Asami, A. Inoue, J. Mater. Res. 17 (3) (2002) 701–704.
- [5] J. Jayaraj, Y.C. Kim, K.B. Kim, H.K. Seok, E. Fleury, Sci. Technol. Adv. Mater. 6 (2005) 256–260.
- [6] V. Ponnambalam, S.J. Poon, G.J. Shiflet, J. Mater. Res. 19 (2004) 1320–1323.
- [7] H. Wang, M.A. Sweikart, J.A. Turner, J. Power Sources 115 (2003) 243–251.
- [8] C.M.A. Brett, A.M. Brett, Electrochemistry: Principles, Methods and Application, Oxford University Press, 1998.
- [9] R.F.A. Jargelius-Pettersson, Corros. Sci. 41 (1999) 1634–1664.